ISSN: 1231-4005
e-ISSN: 2354-0133
DOI: 10.5604/01.3001.0012.4376

INVESTIGATION OF KNOCK SUPPRESSION CHARACTERISTICS IN A BOOSTED METHANE – GASOLINE BLENDED FUELLED SI ENGINE

Zhuyong Yang, Niranjan Miganakallu, Sandesh Rao
Jaideep Harsulkar, Jeffrey Naber

Michigan Technological University
Department of Mechanical Engineering – Engineering Mechanics
1400 Townsend Dr., Houghton MI, U.S.
tel.: +1 906 4871938
e-mail: zhuyongy@mtu.edu

Yashodeep Lonari

Hitachi Automotive Systems Americas, Inc.
34500 Grand River Av., Farmington Hills, MI U.S
tel.: +1 248 4742800
e-mail: yashodeep.lonari@hitachi-automotive.us

Stanislaw Szwaja

Czestochowa University of Technology
Gen. J. H. Dąbrowskiego Street 69, 42-201 Czestochowa, Poland
tel.: +48 34 3250524, fax: +48 34 3250555
e-mail: szwaja@imc.pcz.czest.pl

Abstract

Natural gas has a higher knock suppression effect than gasoline which makes it possible to operate at higher compression ratio and higher loads resulting in increased thermal efficiency in a spark ignition engine However, using port fuel injected natural gas instead of gasoline reduces the volumetric efficiency from the standpoints of the charge displacement of the gaseous fuel and the charge cooling that occurs from liquid fuels. This article investigates the combustion and engine performance characteristics by utilizing experimental and simulation methods varying the natural gas-gasoline blending ratio at constant engine speed, load, and knock level. The experimental tests were conducted on a single cylinder prototype spark ignited engine equipped with two fuel systems: (i) a Direct Injection system for gasoline and (ii) a Port Fuel Injection (PFI) system for compressed natural gas. For the fuels, gasoline with 10% ethanol by volume (commercially known as E10) with a research octane number of 91.7 is used for gasoline via the DI system, while methane is injected through PFI system. The knock suppression tests were conducted at 1500 rpm, 12 bar net indicated mean effective pressure wherein the engine was boosted using compressed air. At 60% of blending methane with E10 gasoline, the results show high knock suppression. The net indicated specific fuel consumption is 7% lower, but the volumetric efficiency is 7% lower compared to E10 gasoline only condition. A knock prediction model was calibrated in the 1-D simulation software GT-Power by Gamma Technologies. The calibration was conducted by correlating the simulated engine knock onset with the experimental results. The simulation results show its capability to predict knock onset at various fuel blending ratios.

Keywords: *knock, methane, gasoline, E10, blend fuel, knock onset prediction, simulation*

1. Introduction

Natural gas production has increased rapidly with the shales gas production [1]. Fig. 1 shows the US annual dry natural gas production since 1930 [2]. An obvious increasing trend can be found

in the recent decade. Besides, natural gas is also known for its widespread availability, economic viability, and environmental benefits [3], making it a promising alternative fuel.

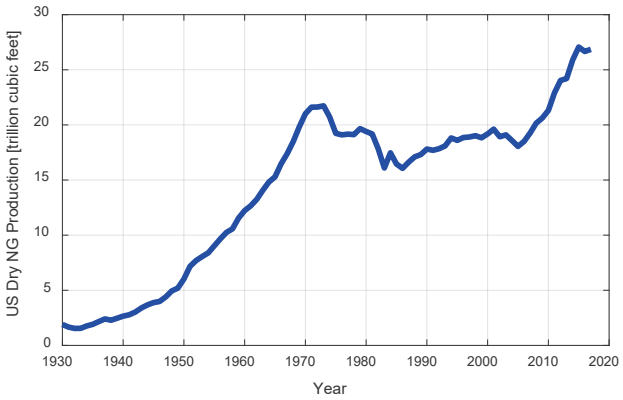

Fig. 1 U.S. Dry Natural Gas Annual Production [2]

The drawbacks of natural gas should also be considered. Energy density of natural gas on a volume basis is much lower compared to gasoline due to its gaseous status. In a port fuel injection system, injecting natural gas instead of gasoline decreases the volumetric efficiency and torque output by over 10% [4]. As a gaseous fuel, natural gas lacks charge-cooling effect, hence peak temperature in the cylinder wall, piston, and valve is much higher. Durability of the conventional gasoline engine is probably insufficient for natural gas [5].

However, increasing the indicated efficiency is one major objective of engine development. In a spark ignition engine, the thermal efficiency is mainly governed by compression ratio but, the sensitivity of engine knock increases with higher compression ratio. Therefore, fuels with higher knock resistance are preferred in extending the engine's efficiency limit.

Based on Naber and Yang et al.'s study [6, 7, 17], and others [17-19] the statistical analysis showed the knock distribution has a positive skew compared to a normal distribution. Both single fuel and blended fuel can be fitted by a log-normal distribution model.

The goal of the current work is to obtain further understanding of the combustion metrics at same knock borderline as a control metric to maintain consistency among different fuel blending ratios. In this article, spark timing was varied by controlling at knock borderline at stoichiometric conditions and retarding it further. Blended fuel used was E10 (gasoline) and methane. Instead of controlling spark timing by a cycle-averaged value, control metric controlled 95th percentile of knock intensity. Further, 1-D simulation was used to predict knock onset. Three knock induction times was calculated to capture the auto ignition among different temperature. The knock model was calibrated at knock borderline. The simulation results showed that the calibrated knock model could estimate the knock onset at different spark timings.

2. Experimental setup

The experiments for this study were conducted at Michigan Technological University's Advanced Power Systems Laboratories (APS Labs) in Houghton, MI US. The engine test cell has a coupled DC and water brake dynamometer for both low and high load control at maximum speeds of 3600 rpm. Previous studies on this engine included ethanol-gasoline blending study by Yeliana et al. [8], residual estimation model development by Vaibhav et al. [9], and water injection study by Miganakallu et al. [10].

Table 1 shows the test engine specifications. It is a single cylinder GM Hydra Engine consisting of two fuel systems with an option of variable cam timing control. Compressed air was also used for boosted conditions.

Tab. 1. Tested Engine Specifications

Bore	86.0 mm
Stroke	94.6 mm
Connecting Rod Length	152.5 mm
Wrist Pin Offset	0.8 mm
TDC Clearance Volume	55931 mm^3
Compression Ratio (CR)	10.93:1 (–)
IVO	-40ºaTDC
IVC	290ºaTDC
EVO	-235ºaTDC
EVC	5ºaTDC
Valve overlap	45º CA

Experimental investigation was conducted with two fuel systems: a direct injection (DI) system for gasoline and a port fuel injection (PFI) system for methane. The gasoline injector was a Bosch HDEV5 DI injector, while the methane injector was a Bosch NGI2 PFI injector.

Two different fuels used in the study are shown in Tab. 2. The lower heating value of E10 gasoline is 41.73 MJ/kg, methane is 50 MJ/kg. The blending ratio (BR) is defined based on the mass fuel flow rate and the lower heating value of these two fuels. The energy based blending ratio is calculated by dividing energy flow rate of methane with the total energy flow rate (E10 gasoline + methane) as given by equation (1):

$$BR\% = \frac{\dot{m}_{methane} \cdot Q_{LHV,\text{methane}}}{\dot{m}_{methane} \cdot Q_{LHV,methane} + \dot{m}_{E10} \cdot Q_{LHV,E10}} \times 100\%. \quad (1)$$

Tab. 2. Fuel specification of E10 gasoline and methane

E10 gasoline	AKI (–)	87.1
	RON (–)	91.7
	MON (–)	82.5
Methane	Purity (%)	99.8

3. Signal processing for knock intensity

Figure 2 shows the schematic of the knock signal acquisition. The knock data acquisition (DAQ) uses an Advantech PCI-1714U card to acquire signals at 250 kHz. A LabVIEW Virtual Instrument was designed to acquire and monitor the knock signal and calculate its statistics in real time. The statistical calculation, which included the 95th percentile, was performed on a moving window of 300 combustion cycles.

Scholl et al. [11] originally investigated engine cylinder pressure signal by using spectrogram to analyse time-dependent frequency content. Fig. 3 shows the engine in-cylinder pressure signal spectrogram of a knock event overlaid with filtered pressure vs. CA. The tested condition was at 20% methane blending ratio for the 95th percentile knock peak-peak. The filtered pressure signal is shown by the red curve in Fig. 3. In Fig. 3, the primary mode of vibration is in 5-8 kHz whereas the secondary mode is in 10-13 kHz. Some smaller contribution is in the frequency range of 14-19 kHz. The spectrum illustrates that the primary and secondary mode of knock signal are well within cut-off frequencies of the band pass filter used in the combustion analyser (ACAP) (4~25 kHz). The knock metric used in this study is knock peak-peak (marked in Fig. 3) which is the peak-peak value of the filtered pressure.

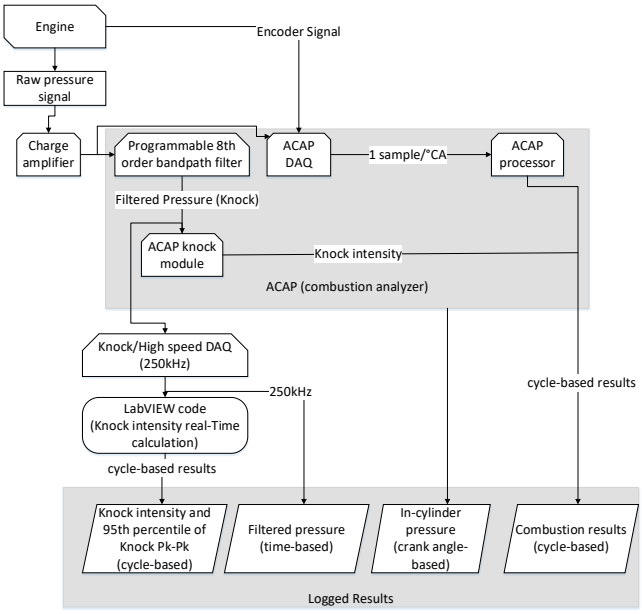

Fig. 2. Schematic of the knock signal processing

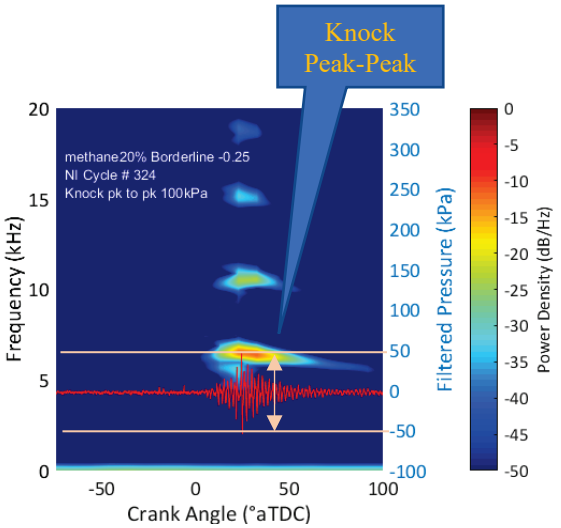

Fig. 3. Cylinder pressure spectrogram with filtered in-cylinder pressure vs. CA

Sinnerstad [12] examined the statistical nature of combustion knock. Naber et al. [6] Utilized 95th percentile of knock as an indicator to normalize knock intensity level. In this study, the knock borderline is defined as the spark timing at which the 95th percentile of the knock dataset exceeds 100 kPa peak-peak of the filtered pressure signal. The 95th percentile was monitored real-time as detailed earlier and was used to identify the knock borderline and maintain statistical consistency with different blending ratios.

4. Test Methodology

The operation point is 1500 rpm/12 bar net indicated mean effective pressure (IMEPnet). The IMEPnet is defined as the piston work of an entire cycle (720ºCA) normalized by the displacement volume. The fuel flow for E10 gasoline and methane was adjusted independently to match the target blend ratios while maintaining stoichiometric combustion. The blending ratios of 60%, 40%, 20% and 0% methane were tested. At blending ratio of 60%, the knock borderline was close to Maximum Brake Torque (MBT) spark timing at 2000 rpm, and hence higher blending ratios were not tested as they would represent lower knock levels than borderline. Data was recorded at the knock borderline and at spark timings around the knock borderline i.e. after finding the knock borderline the spark timing was retarded to 0.75ºCA in steps of 0.25ºCA. At 0.75ºCA after knock borderline, knock peak-peak at 95th percentile was significantly lower and retarding the spark timing further would result in no knock being observed, and hence the spark retarded was limited to 0.75ºCA. Details of the experimental conditions are provided in Tab. 3.

5. Experimental results and discussion

The results in this section are the averaged values at each test point for the 300 logged cycles. Each blending ratio includes four different spark timing conditions as explained above and given in Tab. 3. Methane BR 80 and 100% were only performed once since no knock occurred for the crank angle of 50% of fuel mass faction burned (CA50) at 8ºaTDC. Fig. 4 shows the CA50 of different methane blending ratio and spark timing. As the methane blending ratio increased, borderline spark timing was much closer to the maximum brake torque (MBT) spark timing. The CA50 of E10 only condition (BR0%) was at 24ºATDC to obtain the borderline spark timing.

At methane BR60%, knock borderline spark timing was at CA50 8°, and hence higher blending ratios were not tested with a spark timing sweep as lower knock levels would be achieved. Fig. 5 shows the results of the 95th percentile of knock peak-peak vs CA50. For the same blending ratio, a retarded spark timing resulted in a retarded in CA50 and lower knock level. Compared to the borderline spark timing, the 95th percentile of knock peak-peak was reduced by 40% at borderline -0.75ºCA.

Tab. 3 Experimental conditions

Engine speed	1500 rpm
Load	12 bar IMEPnet
Knock borderline	95th percentile of peak-peak = 100kPa
Methane blending ratio	0 / 20% / 40% / 60%
Spark timing	Borderline + 0, -0.25, -0.50, -0.75°CA ("-" indicates retard)
DI SOI	300º before firing TDC
PFI SOI	330º before firing TDC
DI pressure	10 MPa
PFI pressure	0.4 MPa
Number of cycles	300
COV of IMEP limit	5%

Volumetric efficiency was calculated based on the manifold temperature and pressure as given by equation (2):

$$\eta_{vol} = \frac{2\dot{m}_{manifold}}{\rho_{manifold}\, V_d\, N}. \tag{2}$$

where:
$\dot{m}$ – the mass flow rate of air through the manifold,
ρ – the air density in the manifold,
V_d – the engine displacement,
N – the engine speed.

It is expected that volumetric efficiency would decrease as methane was supplied from a PFI injector. Fig. 6 shows volumetric efficiency of gasoline only condition was at 87%. As the blending ratio was increased to 60%, volumetric efficiency was decreased to 79%. In Fig. 7, MAP BR60% is 3 kPa higher than BR40%. MAP of BR20% and BR0% was around 1 kPa higher than BR40%. Fig. 8 is the coefficient of variance (COV) of IMEPnet vs. CA50. A much stable IMEPnet was observed during higher methane blending ratio. The results are in agreement with the log-normal distribution model developed by Naber and Yang et al. [6, 7]. In the log-normal distribution model, the coefficient of σ describes the variance of samples. The coefficient of σ is lower at higher methane blending ratios.

Crank angle between fuel burned mass fraction at 0% and 10% (burn duration 0-10%) decreased as the methane blending ratio was increased from BR0% to BR40%. As the combustion phasing become more advanced, higher in-cylinder temperatures leads the early flame propagation much faster. However, Burn Duration (BD) 0-10% at BR60% is closed to level of BR0%. One conceivable scenario is the different turbulence among different blending ratios. E10 gasoline was supplied by a DI injector. Different amount of E10 may affect the turbulence in the engine cylinder. At methane BR60%, injected E10 was much lower than methane BR0%, which leads to lower turbulence and longer BD 0-10%.

Research by Sevik et al. [13] shows natural gas combustion duration 10%-90% (BD 10%-90%) is longer than E10 gasoline. BD 10%-90% in Fig. 10 is in agreement with the research conducted

by Sevik et al. It shows the BD 10%-90% at knock borderline is increased as the methane blending ratio increasing.

Indicated net specific fuel consumption in Fig. 11 is calculated by the equation (3):

$$NSFC_{equivalent,tot} = \sum NSFC_{test\ fuel,i} \times \frac{LHV_{test\ fuel,i}}{LHV_{E10}}. \quad (3)$$

The fuel consumption is scaled by the factor of lower heat value ratio between different fuels. As the knock resistance is higher at higher BR, combustion phasing was able to be closer to MBT condition governed the NSFC of BR60% 7% lower compared to the condition of BR0%. The NSFC of BR80% and BR100% is much lower, but the knock no longer occurred.

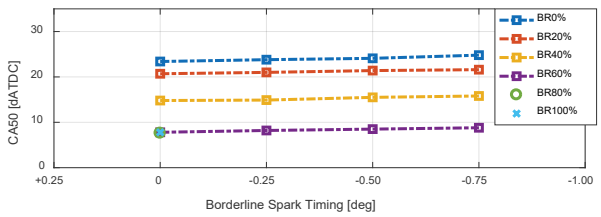

Fig. 4. CA50 vs. spark timing at 1500 rpm, 12 bar IMEPnet

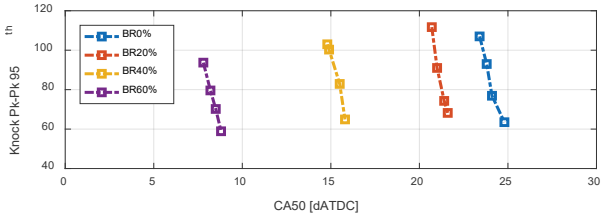

Fig. 5. Knock peak-peak 95th percentile vs. spark timing at 1500 rpm, 12 bar IMEPnet

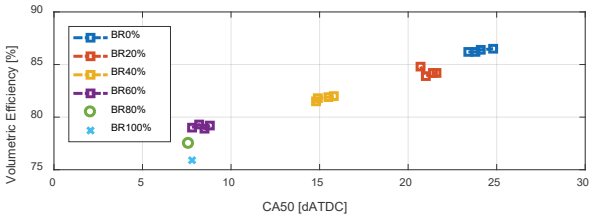

Fig. 6. Volumetric vs. spark timing at 1500 rpm, 12 bar IMEPnet

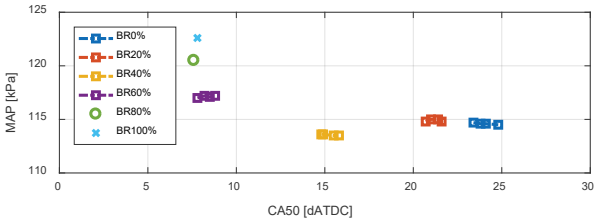

Fig. 7. MAP vs. spark timing at 1500 rpm, 12 bar IMEPnet

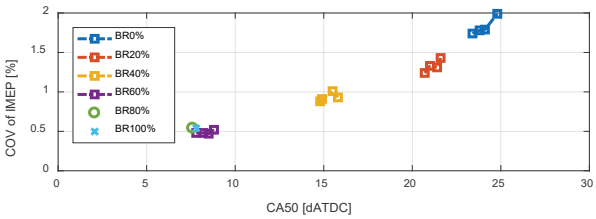

Fig. 8. COV of IMEP vs. spark timing at 1500 rpm 12 bar IMEPnet

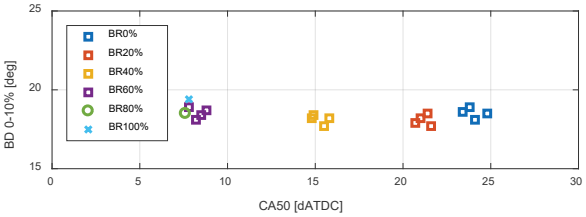

Fig. 9. Burn duration 0-10% vs. spark timing at 1500 rpm, 12 bar IMEPnet

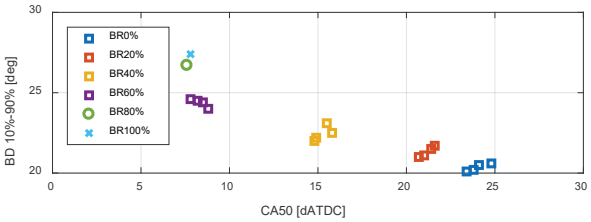

Fig. 10. Burn duration 10-90% vs. spark timing at 1500 rpm, 12 bar IMEPnet

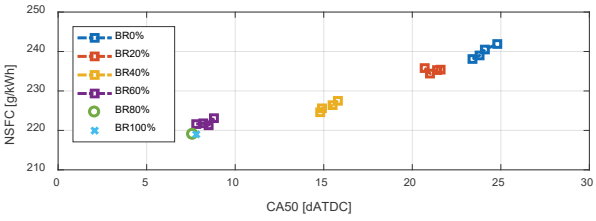

Fig. 11. $NSFC_{equivalent}$ vs. spark timing at 1500 rpm 12 bar IMEPnet

6. Knock onset prediction by 1-D simulation

In the current work, the engine has been modelled using the 1-D simulation software GT-Power by Gamma Technologies. The model was calibrated at knock borderline spark timing

at each blending ratio. It has been primarily used to validate the knock onset at different spark timings.

The combustion model is the SI Turbulence model. The knock onset model used is a chemical kinetic model, Kinetics Fit (KF) model [14] based on detailed kinetics simulation by Ra and Reitz. This model uses three induction times to capture the different chemistry of auto-ignition over a wide range of temperature. The overall induction time, τ, is given by [15]:

$$\tau_i = M_1 a_i \left(\frac{ON}{100}\right)^{b_i} [Fuel]^{c_i} [O_2]^{d_i} [Diluent]^{e_i} \exp\left(\frac{f_i}{M_2 T}\right). \quad (4)$$

Where M_1 is the knock induction time multiplier, ON is the octane number of the fuel, M_2 is the activation energy multiplier, [Fuel], [O2] and [Diluent] are concentrations expressed in mol/m^3 while a_i to f_i are model constants [15]. The model predicts the onset of knock at a crank angle where the induction time integral at any end gas zone attains a value of 1.0. Thus, for calibration and validation of the knock model, octane number and the fuels are specified as the input whereas the parameters M_1 and M_2 have been tuned for accurate modelling of the engine under knocking conditions.

The model was calibrated by the cycle of 95th percentile of knock peak-peak at knock borderline from the experimental results. Calibrated test conditions were at knock borderline for each blending ratios. The calibrated points are shown here in Tab. 4,

Tab. 4 Calibrated Points for Knock Onset Prediction

Calibrated cycle	Spark timing	Methane blending ratio (%)	Knock onset observed from experiment	Knock induction time multiplier	Activation energy multiplier
95th percentile of knock peak-peak	Knock borderline	0	26	0.96	3.9
		20	23	0.975	3.8
		40	20	0.0062	1.0
		60	13	4.7	1.5

Comparison of the results in Fig. 12 shows that the model has been calibrated with maximum error of 2.0ºCA for onset of knock. Referring to an earlier work done in prediction of knock onset by Pipitone et al. [16], where the accuracy was ±3.5ºCA for knock onset prediction. The error obtained in the current model is lower than the maximum acceptable error determined by Pipitone et al. Hence, the error in the current project has been described as being acceptable.

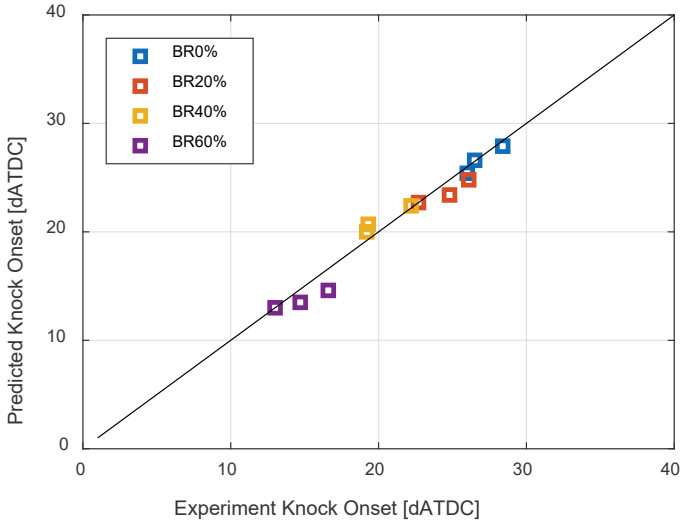

Fig. 12 Predicted knock onset vs. experiment knock onset

The trend for both the operating conditions suggests an earlier onset of knock with increasing natural gas blending ratio. This can be explained by the fact that with an increase in blending ratio, higher knock resistance is achieved and thus the spark advance needs to be advanced to close to MBT.

Since the simulated model is able to predict the onset of knock for different spark timing at the respective operating conditions within an acceptable error it can be concluded that the GT-Power model developed has been successfully calibrated and validated. This model can be used to predict the onset of knock at spark timing close to knock borderline for a similar operating condition. Further analysis of the knock onset prediction at different blending ratio is suggested.

7. Summary and Conclusions

This study provided an overview of knock suppression characteristics based on constant speed/load and knock level with DI E10 gasoline and PFI methane fuels. Knock tests with a borderline spark timing sweep was conducted at methane blending ratios of 0, 20, 40 and 60% at an engine speed 1500 RPM and $IMEP_{net}$ of 12 bar. The volumetric efficiency decreases as the NG blending ratio increases. With higher blending ratio, more gaseous fuel and less air are inducted in the engine cylinder, which leads to lower volumetric efficiency. MAP does not remain constant during the sweep of BR. MAP was decreased from BR100% to BR40%. MAP at BR40% to BR0% does not show significantly change. The trend of MAP increased at lower BR probably due to its higher specific fuel consumption compare to higher BR under the stoichiometric condition.

COV of IMEPnet was at 0.5% at BR60%. An increase in the blending ratio resulted in a decrease in the COV of IMEP. The higher variance of COV at lower BR is in agreement with the statistic analysis in previous work [7].

BD 0-10% decreased as the BR increased from BR0% to BR20%. As the spark timing is much more advanced, higher in-cylinder temperature governs the faster earlier flame propagation. At higher BR, BD 0-10% does not keep decreasing. A conceivable scenario is the lower turbulence in the cylinder as lesser E10 gasoline was supplied from the DI injector.

BD 10-90% was increased as the BR was increased. The longer BD 10-90% is mainly due to the slower flame speed of methane as the BR of methane was increased.

Indicated net specific fuel consumption is lower at high BR conditions. As the knock resistance is higher at higher BR, combustion phasing was closer to MBT condition. The NSFC is 7% lower compared to E10 only condition.

The engine was modelled for knock onset using GT-Power. Kinetics Fit model was implemented and calibrated at knock borderline of each blending ratios. It was found that the model is able to predict onset of knock within an error of ±2ºCA. The trend observed suggested an earlier knock onset with an increase in the blending ratio due to higher knock resistance. Since the model results closely correlated with the experimental results at different blending ratios, it can be concluded that the model has been successfully validated for the given SI engine and the given operating conditions.

Acknowledgements

This project has partially received funding from the European Union's Horizon 2020 research and innovation programme under grant agreement No 691232 – Knocky – H2020-MSCA-RISE-2015/H2020-MSCA-RISE-2015.

References

[1] King, G. E., *Thirty years of gas shale fracturing: What have we learned?*, in SPE Annual Technical Conference and Exhibition, Society of Petroleum Engineers, 2010.

[2] EIA, *Natural gas annal*, U.E.I. Administration, 2017.
[3] Srivastava, D. K., Agarwal, A. K., *Comparative experimental evaluation of performance, combustion and emissions of laser ignition with conventional spark plug in a compressed natural gas fuelled single cylinder engine*, Fuel, Vol. 123, pp. 113-122, 2014.
[4] Wayne, W. S., Clark, N. N., Atkinson, C. M., *A parametric study of knock control strategies for a bi-fuel engine*, SAE International, 980895, 1998.
[5] Kato, K., Igarashi, K., Masuda, M., Otsubo, K., et al., *Development of engine for natural gas vehicle*, SAE International, 1999-01-0574, 1999.
[6] Naber, J., Blough, J. R., Frankowski, D., Goble, M., et al., *Analysis of combustion knock metrics in spark-ignition engines*, SAE Technical Paper, 2006-01-0400, 2006.
[7] Yang, Z., Rao, S., Wang, Y., Harsulkar, J., et al., *Investigation of combustion knock distribution in a boosted methane: gasoline blended fueled SI engine*, SAE International, 2018-01-0215, 2018.
[8] Yeliana, Y., Cooney, C., Worm, J., Michalek, D. J., et al., *Estimation of double-Wiebe function parameters using least square method for burn durations of ethanol-gasoline blends in spark ignition engine over variable compression ratios and EGR levels*, Applied Thermal Engineering, Vol. 31 (14), pp. 2213-2220, 2011.
[9] Kale, V., Yeliana, Y., Worm, J., Naber, J. D., *Development of an improved residuals estimation model for dual independent cam phasing spark-ignition engines*, SAE International, 2013-01-0312, 2013.
[10] Miganakallu, N., Naber, J. D., Rao, S., Atkinson, W., et al., *Experimental investigation of water injection technique in gasoline direct injection engine*, (58318), V001T03A013, 2017.
[11] Scholl, D., Barash, T., Russ, S. Stockhausen, W., *Spectrogram analysis of accelerometer-based spark knock detection waveforms*, SAE Technical Paper, 972020, 1997.
[12] Sinnerstad, K., *Knock intensity and torque control on an SVC engine*, Institutionen för Systemteknik, 2004.
[13] Sevik, J., Pamminger, M., Wallner, T., Scarcelli, R., et al., *Performance, efficiency and emissions assessment of natural gas direct injection compared to gasoline and natural gas port-fuel injection in an automotive engine*, SAE International Journal of Engines, Vol. 9, pp. 1130-1142, 2016.
[14] Ra, Y., Reitz, R. D., *A combustion model for IC engine combustion simulations with multi-component fuels*, Combustion and Flame, Vol. 158 (1), pp. 69-90, 2011.
[15] Manual, G.-P.U.s., *GT-Suite version 2016*. Gamma Technologies Inc, 2016.
[16] Pipitone, E., Genchi, G., Beccari, S., *An NTC zone compliant knock onset prediction model for spark ignition engines*, Energy Procedia, Vol. 82, pp. 133-140, 2015.
[17] Naber, J. D., Szwaja, S., *Statistical approach to characterise combustion knock in the hydrogen fuelled SI Engine*, Journal of KONES Powertrain and Transport, Vol. 14, No. 3, pp. 443-450, Warsaw 2007.
[18] Szwaja, S., Naber, J. D., *Impact of leaning hydrogen-air mixtures on engine combustion knock*, Journal of KONES Powertrain and Transport, Vol. 15, No. 2, pp. 483-492, Warsaw 2008.
[19] Szwaja, S., Naber, J. D., *Exhaust gas recirculation strategy in the hydrogen SI engine,* Journal of KONES Powertrain and Transport, Vol. 14, No. 2, pp. 457-464, Warsaw 2007.

Manuscript received 04 May 2018; approved for printing 27 August 2018